SUPPLEMENTARY INFORMATION

Supplementary Methods

Design and Construction of Plasmids. Most constructs were assembled whole by two-step overlap PCR and subcloned into the mammalian vector pcDNA3 or a modified version with a truncated SV40 promoter (10-fold lower expression relative to CMV). Unique cut-sites flanked most fused domains such that some constructs were assembled by replacing signalling domains via standard subcloning. (Complete plasmid sequences are available upon request.)

Table S1 Plasmids		
pAL113	pCMV-PhyBNT(Y276H)-10aaLinker-mCFP-HrasCT	Fig. S1
pAL161	pCMV-PhyB(1-450)-10aaLinker-mCherry-Kras4BCT	Fig. 1c
pAL117	pCMV-PhyB(1-650)-10aaLinker-mCherry-Kras4BCT	Fig. 1c
pAL148	pCMV-PhyB(1-650)-Gal4DD-10aaLinker-mCherry-Kras4BCT	Fig. 1c
pAL149	**pCMV-PhyB(1-908)-10aaLinker-mCherry-Kras4BCT**	~All Figs, Movies 1-9
pAL162	pCMV-PhyBFL-10aaLinker-mCherry-Kras4BCT	Fig. 1c
pAL140	pCMV-PhyA(1-650)-10aaLinker-mCherry-Kras4BCT	Fig. 1c
pAL139	pCMV-mYFP-Fhy1CT	Fig. 1c
pAL138	pCMV-PIF3APA-mYFP	Fig. 1c
pAL130	pCMV-PIF3NT-mYFP	Fig. 1c
pAL100	pCMV-PIF3APB-mYFP	Fig. 1c
pAL101	pCMV-PIF6APB-mYFP	Fig. 1c,4b
pAL175	pΔSV40-mYFP-PIF6APB	Fig. 2,3,S2 Movies 1-6,10
pAL167	pCMV-TiamDHPH-20aaLinker-mYFP-PIF6APB	Fig. 4b
pAL188	pΔSV40-TiamDHPH-20aaLinker-mYFP-PIF6APB	Fig. 4c Movies 7,8
pAL189	pΔSV40-IntersectinDHPH-20aaLinker-mYFP-PIF6APB	Fig. 4d Movie 11
pAL190	pΔSV40-TimDHPH-20aaLinker-mYFP-PIF6APB	Movie 9
pAL197	pΔSV40-PakGBD-mCherry	Fig. S4
pAL198	pΔSV40-mCherry-WaspGBD	Fig. 4d Movie 11
pAL204	pCMV-PhyB(1-908)-10aaLinker-mCFP-Kras4BCT	Fig. 4d Movie 11

Phytochrome, PIF domains PhyB-CBD (PhyB450NT), PhyB-NT (PhyB650NT), PhyB-908NT, and PhyB-FL domains were amplified by PCR from vector PhyBFL-GBD; this vector contains full-length phyB [Entrez Gene ID: 816394] cDNA from Arabidopsis thaliana. PhyA-NT (1-650) was cloned from previously subcloned cDNA. PIF3NT, PIF3APA (aa120-210),PIF3APB (PIF3-100NT) and PIF6APB (PIF6-100NT) domains were amplified by PCR from vectors PIF3-GAD and PIF6APB, respectively; these vectors contain subsequences of the PIF3 [Entrez Gene ID: 837479] and PIF6 [Entrez Gene ID: 825382] genes from Arabidopsis thaliana. All three vectors were gifts from Peter Quail. Arabidopsis Fhy1CT(117-202) [Entrez Gene ID: 5007942] was amplified from Arabidopsis thaliana cDNA.

Linker domains The linker domains used are standard polyglycine-serine flexible linkers and were made by oligo annealing: 10aa-linker: DSAGSAGSAG [gat agt gct ggt agt gct ggt agt gct ggt], 20aa-linker: SAGGSAGGSAGGSAGGSAGG [agt gct ggt ggt agt gct ggt ggt agt gct ggt ggt agt gct ggt ggt agt gct ggt ggt]

Dimerization domain The Gal4 dimerization domain[1] (residues 50-106) was cloned from a *Saccharomyces cerevisiae* cDNA library.

Localization domains Small C-terminal localization tags were created by oligo annealing: Hras [Entrez Gene ID: 3265] palmitoylation CaaX sequence (GCMSCKCVLS), [ggc tgc atg agc tgc aag tgt gtg ctc tcc], Kras4B [Entrez Gene ID: 3845] polybasic CaaX terminus (KKKKKKSKTKCVIM) [ggt aaa aag aag aaa aag aag tca aag aca aag tgt gta att atg]

Fluorescent Proteins mCFP and mYFP (ECFP and EYFP with monomerizing A206K mutation) were amplified by PCR from Invitrogen vectors. mCherry was amplified by PCR from vector supplied by Rogen Tsien.

RhoGEFs DHPH domains from human RhoGEFs Tiam [Entrez Gene ID: 7074], Intersectin [Entrez Gene ID: 6453], and Tim [Entrez Gene ID: 7984] were amplified by PCR from vectors carrying previously subcloned copies of these cDNAs.

Mammalian Promoters The standard CMV promoter from the pcDNA3 vector was used in most constructs. In some plasmids a truncated sv40 promoter was used instead to lower expression levels of recruitee constructs in transiently transfected cells (10-fold lower expression than CMV).

Phycocyanobilin (PCB) Purification. 50g *Spirulina* powder (Seltzer Chemical) was resuspended in 1.5L doubly distilled water (30mL/g), stirred for 10minutes, then spun at 8000rpm at 4°C for 1 hour. The dark green cell pellet was discarded and the cyan supernatant was treated with 15g TCA (1% w/v) to precipitate soluble protein. This solution was stirred at 4°C in the dark for an hour then spun at 8000rpm at 4°C for 10 minutes. The pellet was resuspended and washed three times by adding 1.5L methanol and spinning at 8000rpm for 10 minutes at 4°C to remove free tetrapyrroles (repeated until supernatant was clear). Great care was taken from this point on to shield the free PCB-containing mixtures from all light by wrapping glassware in aluminum foil or by using a green safelight (Sylvania F40G fluorescent tube wrapped once with a Roscolene 874 sheet and once with a Roscolene 877 sheet, 550nm) in a darkroom. The washed cyan pellet was collected and subjected to methanolysis in 500mL methanol by refluxing at 70°C for eight hours. To increase the yield the remaining pellet was subjected to a second, identical methanolysis for a second pool that was further handled in parallel with the first. Each methanolysis extraction was evaporated to 50mL using a roto-evaporator.   This concentrated PCB solution was extracted twice with 50mL chloroform and 100mL water, the chloroform layers were removed with a separatory funnel and dried with a roto-evaporator to a dry residue. The residue was resuspended in 3mL DMSO, aliquoted and

stored at -80°C. The final PCB concentration was quantified by spectroscopy by diluting the

DMSO stock 1:100 into 1mL MeOH:HCl(37.5%) 95%:5% solution and reading the absorbance

at 680nm. The concentration in mM was calculated as A680 x 2.64, typical final concentrations

were 3-15mM.

Cell culture and transfections. NIH3T3 cells were obtained from ATCC and maintained in

DMEM supplemented with 10% (v/v) BCS, glutamine, and antimicrobials at 37°C in a

humidified, CO2-controlled (5%) incubator.   For experiments, 120,000 NIH3T3 cells were

plated on poly-d-lysine coated glass-bottomed petri dishes (Mattek) before transfection.

Transfections were performed with Lipofectamine 2000 (Invitrogen) at a 3:1 μL/μg ratio of

reagent to DNA, mixed in Optimem (Invitrogen) for 25 minutes and added directly to cells for

five hours before washing reagent out with serum-containing media. Microscopic observations

took place at least twelve hours post-transfection. Serum depletion was performed where

indicated by dilution of serum-containing media by DMEM supplemented with 1% (w/v) fatty-

acid free BSA, followed by at least six hours of depletion. PCB was added to cells under green

safelight at least half an hour before experiments by prediluting the concentrated DMSO stock in

BSA-supplemented DMEM and then adding to cells for a final concentration of 5μM. This

weakly fluorescent PCB-containing media was swapped immediately before imaging with

mHBSS [150mM NaCl, 4mM KCl, 1mM MgCl2, 10mM glucose, 20mM Hepes pH 7.2]

supplemented by 1% fatty-acid free BSA.

Global Recruitment Assays. Global recruitment assays were performed at 37°C on a spinning

disk confocal microscope consisting of a Nikon TE2000-U inverted microscope surrounded by a

temperature-control chamber, equipped with a Yokogawa CSU22 confocal scanning unit

(Solamere Technology Group) using Ar and Ar/Kr laser lines at 568nm, 488nm and emission

filters for YFP and mCherry (Nikon 100x Apochrom 1.49NA). Images were captured with a

Photometrics Cascade II EMCCD camera. Cells were exposed to activating or deactivating

wavelengths by filtering brightfield light with either a 650nm 20nm-bandpass filter (Edmund

Optics) or a near-IR RG9 glass filter (Newport). Total photon fluence was measured at the sample plane by using a portable calibrated fiber-optic spectroradiometer (EPP2000C, Stellarnet Inc). To measure kinetics of recruitment and release, cells were exposed to fixed periods of red or infrared light, the PIF-YFP distribution was imaged, then the Phy-PIF pool was returned to fully-recruited or fully-released equilibrium by exposure to 10s of the opposite wavelength of light, then exposed again for a longer fixed period of the original wavelength in a loop. Such iterative measurements are necessary to eliminate the strong activating perturbations induced by the imaging light itself. The different nuclear concentrations of PIF-YFP in the panels of figure 2 are a result of passive nuclear partitioning: cells initialized to the "ON" state gradually deplete the nucleus of PIF-YFP through continuous cytoplasmic depletion, cells initialized to the "OFF" state have their nucleus filled by passive diffusion from a PIF-YFP rich cytoplasm.

Localized Recruitment and Signal Induction. Localized recruitment assays were performed at 37°C using total internal reflectance (TIRF) microscopy on a Nikon TE2000E inverted microscope surrounded by a temperature-control chamber, equipped with a Nikon laser TIRF illuminator (Nikon 60x Apochrom 1.49NA). Ar laser lines 488nm, and 514nm and solid state 561nm lasers were used through a LEP MAC5000 shutter system. Images were collected with a Photometrics Cascade II EMCCD camera. Local induction was performed with a MicroPoint microscope laser system (Photonic Instruments) using a pulse UV-pumped Rhodamine 650nm dye cell laser. The illumination point was made parfocal with microscope optics by test-ablation of a metal-sputtered glass slide. To locally recruit fluorescently tagged signalling factors, continuous 20Hz pulses of the 650nm light at low intensity were centered on a patch of plasma membrane while simultaneously irradiating the whole cell with inhibitory IR light from a brightfield source at maximal intensity filtered by an RG9 IR long-pass glass filter (Newport). For detection of recruited fluorophore, TIRF imaging is necessary as wide-field (EPI) is unable to distinguish cytoplasmic vs. membrane-recruited fractions in thin cellular regions.

Patterned Membrane Recruitment Recruitment of YFP-tagged APB to patterned regions of the cell membrane was performed at room temperature using total internal reflectance (TIRF) microscopy on a Nikon TE2000E inverted microscope equipped with a Nikon laser TIRF illuminator (Nikon 60x Apochrom 1.49NA). Ar laser lines 488nm, and 514nm and solid state 561nm lasers were used and emission light filtered by a Sutter Lambda 10-3 Filter Wheel. Images were collected with a Photometrics Cascade II EMCCD camera. To produce patterned Red/IR profiles at the cell surface, alternating 650nm and 750nm light was produced using 20nm bandpass filters (Chroma) with a broad-spectrum arclamp in a Lambda DG-4 source. These wavelengths were patterned by use of a commercial digital micromirror device brought into a conjugate focal plane with the sample. (Mosaic Digital Diaphragm, Photonic Instruments) The illumination frequencies were switched at the maximum update speed for the device, which was roughly 8Hz. Illumination, acquisition and light patterning of the glider motif were orchestrated by a custom script written in Metamorph.

Morphological Induction Assays. Morphology induction assays were performed by exposing cotransfected, PCB-preincubated (30min) or PCB-free control cells to red light while observing on a Nikon TE2000E inverted microscope in widefield with a 514/561 dichroic mirror and YFP and mCherry channel emission light filtered by a Sutter Lambda 10-3 Filter Wheel. Images were collected with a Photometrics Cascade II EMCCD camera. The constructs were scored by counting the percentage of cotransfected cells exhibiting lamellipodia within the twenty-minute observation window.

Spot Titration and TIRF Recruitment Biosensor Assays. Localized TIRF biosensor recruitment assays were performed at RT using total internal reflectance (TIRF) microscopy on a Nikon Ti inverted microscope equipped with a Nikon laser TIRF illuminator (Nikon 100x Apochrom 1.49NA). Ar laser lines 488nm, and 514nm and solid state 440nm, 561nm lasers were used through a LEP MAC5000 shutter system. Images were collected with a Andor iXon EMCCD camera. Local induction was patterned by use of a commercial digital micromirror

device brought into a conjugate focal plane with the sample. (Mosaic Digital Diaphragm,

Photonic Instruments) This micromirror array device was custom modified to allow two input

light sources such that both 'on' and 'off' mirror states were used to reflect 650nm and 750nm

light into the optical axis of the microscope simultaneously.

Supplemental Calculation Membrane Capture Time Constant for Perfect Spherical Absorber

An approximate time constant for capture of molecules diffusing in a cell with diffusion constant D to a perfectly absorbing spherical membrane (radius R) can be easily calculated by solving the poisson equation for the "mean-first-capture-time field".[2]

Mean time equation for a particle encountering a non-attracting boundary for the first time by diffusion (diffusion constant D):

$$D \Delta W + 1 = 0$$

W is mean time to encounter (shown by electrostatic analogy). Solving this equation for the inside of a spherical cell of radius R yields a solution of the form:

$$B - A/r - r^2/(6D)$$

Boundary conditions (mean-capture-time at r=R is zero, continuity requires derivative must be zero at origin) fix constants for a solution:

$$(R^2 - r^2)/(6D)$$

Averaging this value over the inside of the spherical cell yields an approximation for the time constant for membrane capture:

$$R^2/(15D)$$

For typical cell values: (20μm cell diameter, 30μm^{2}s^{-1} D for cytoplasmic GFP) this equals **.22 seconds.** Given that this calculation assumes capture at the *first* membrane-encounter it serves as a lower bound.

Supplemental Movies

1 YFP membrane recruitment Cytosolic PIF-YFP is recruited onto the membrane by PhyB under the action of 650nm light. A confocal slice of a NIH3T3 cell is shown.

2 YFP membrane dissociation Membrane-bound PIF-YFP is released back to the cytosol by PhyB under the action of >750nm light. A confocal slice of a NIH3T3 cell is shown.

3 oscillating YFP translocation The photostability of the system is shown by repeated rounds of recruitment and release of PIF-YFP to and from the membrane by PhyB under action of oscillating 650nm and IR (>750nm) light.

4 YFP point recruitment PIF-YFP is recruited to a single, moving point by action of a focused 650nm laser with global inhibition by >750nm irradiation. The membrane of a NIH3T3 cell is shown using TIRF microscopy.

5 patterned recruitment of YFP PIF-YFP is recruited in a patterned fashion to the plasma membrane. Sequential frames of a movie of a "glider" pattern from the "game of life" cellular automaton is projected onto the membrane as an inverse R/IR light distribution. The membrane of a NIH3T3 cell is shown using TIRF microscopy.

6 titrated recruitment of YFP PIF-YFP is recruited to a circular region on the plasma membrane. The time-average ratio of 650nm-reflecting pixels from the micromirror array is steadily increased by dithering the illumination mask with rapidly updating white noise with pixel densities that increase with each frame (resulting in a steady time average increase). The amount of Pfr PhyB, and thus recruited YFP is thereby titrated.

7 cell extrusion by Tiam(Rac GEF) recruitment An extended process from a cell is induced and guided by locally stimulating Rac1 via membrane-recruited Tiam(Rac GEF) DHPH. A NIH3T3 cell is shown using standard epifluorescence microscopy.

8 dynamic lamellipodia by Tiam(Rac GEF) recruitment Lamellipodia are induced and released on a physiological timescale by local Tiam(Rac GEF) recruitment, showing the quick responsiveness of the system. A NIH3T3 cell is shown using standard epifluorescence microscopy.

9 periodic contractions by Tim(Rho GEF) recruitment Alternating global irradiation of NIH3T3 cells transfected with a Tim (Rho GEF) DHPH recruitee construct causes rhythmic contractions of the cell tightly coupled to the light condition. A NIH3T3 cell is shown using standard epifluorescence microscopy.

10 PIF-YFP only recruitment control This movie shows the typical result that pif-YFP recruitment alone does not seem to produce any detectable polymerization or ruffling activity in the cytoskeleton. (Such spurious morphological effects have not been seen in any of our YFP-only system characterization experiments.)

11 monitoring membrane-bound Cdc42-GTP dynamics via recruited mCherry-WASP-GBD in TIRF A small circular region of a NIH3T3 cell's plasma membrane is illuminated off and on with red light. Phy-pif recruitment of IntersectinDHPH to the plasma membrane causes it to bind and activate Cdc42 by inducing nucleotide exchange to the GTP bound form. The WASP GBD domain specifically recognizes this form and is preferentially recruited to regions of high Cdc42-GTP content. By exploiting this fact in TIRF mode we can monitor the downstream effects of GEF activity in NIH3T3 cells.

Supplemental References

1. Hidalgo *et al*. Recruitment of the transcriptional machinery through GAL11P: structure and interactions of the GAL4 dimerization domain. *Genes Dev* **15,** 1007-20 (2001).

2. Berg, Howard C. Random Walks in Biology. Princeton University Press (1993).
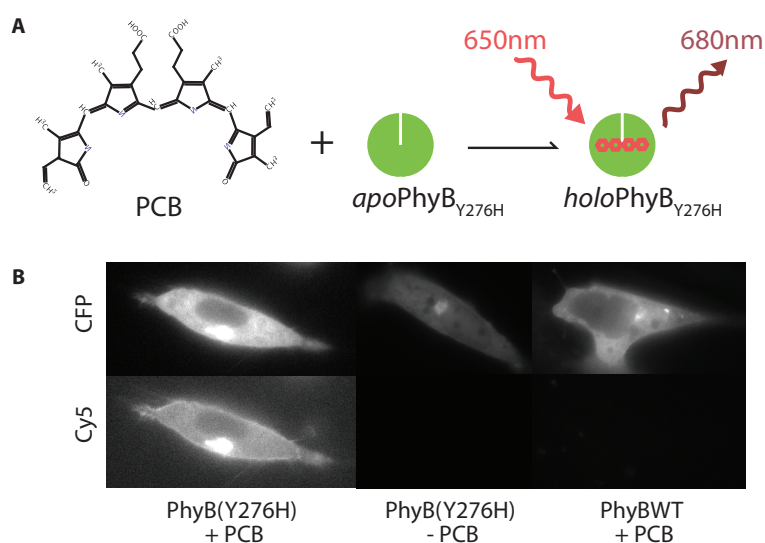
Figure S1 PhyB-PCB holoprotein formation was tested in live mammalian cells by epi-fluorescence microscopy. **A** PhyB Y276H mutant forms a bright far-red fluorophore upon conjugation to PCB chromophore. Free PCB and wildtype holoprotein are only very weakly fluorescent. **B** Images of CFP-tagged membrane-localized phytochrome constructs in NIH3T3 cells. PCB-free and wildtype PhyB controls show no fluorescence above background in Cy5 channel, whereas PhyB(Y276H) pre-incubated with PCB shows bright membrane localized fluorescence after 30min 5μM PCB incubation at 37C, showing rapid formation of holoprotein in living cells at standard conditions.
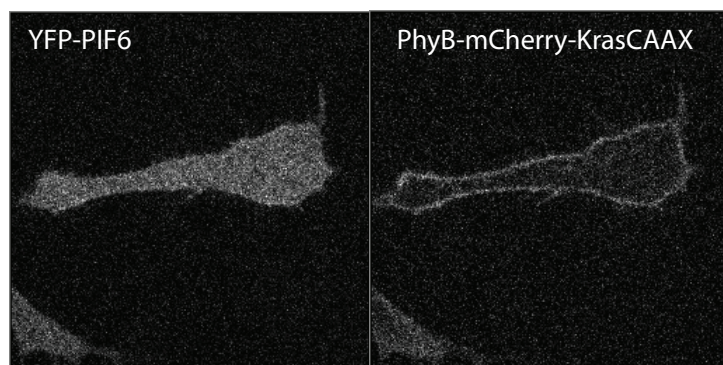

Figure S2 Confocal images of unrecruited YFP-PIF6apb and PhyB908-mCherry-KrasCAAX constructs showing their respective (uninduced) cytosolic and plasma-membrane localizations in NIH3T3 cells a day post-transfection.
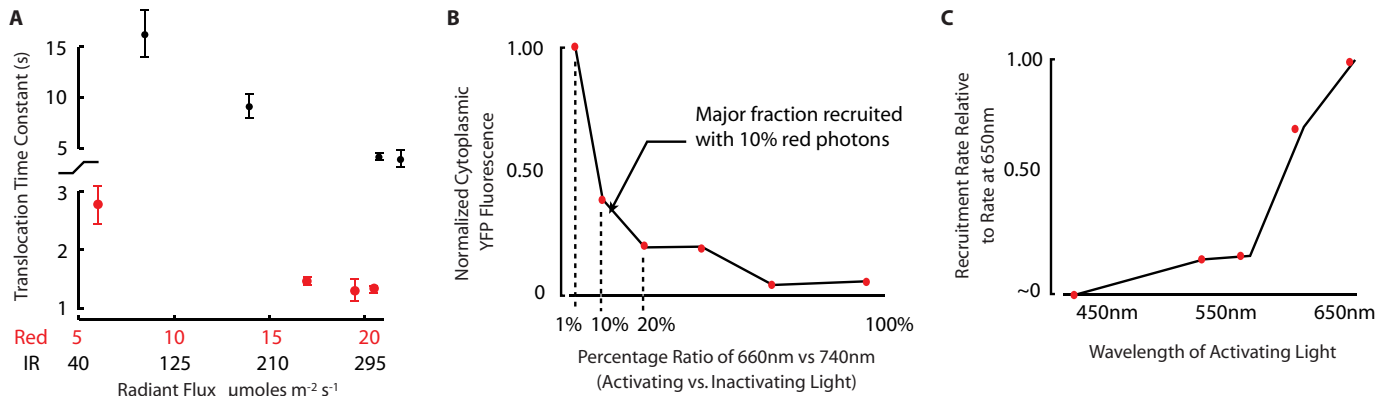
Figure S3 Quantitative characterization of the effects of light strength and quality were measured for the PhyB908-PIF6APB pair. **a**, The photon flux was titrated to test for saturation of the phytochrome pool. For red light, saturation appears to occur at around 20 µmoles m^{-2} s^{-1}, even laser activation (with significantly higher fluxes) does not speed membrane translocation. For infrared reverse stimulation it is not clear that saturation occured with the low intensity infrared sources used in our experiments. Stronger infrared light (for instance, in 2-photon microscopy) could drive even faster "OFF" kinetics and tighten the ultimate spatial resolution of recruitment. (error bars s.e.m., n=3) **b**, The fraction of red photons in combined red and infrared illumination necessary to activate the phytochrome pool was measured by varying intensities of calibrated LEDs at 640nm and 740nm. A 10% fraction of red light was sufficient to activate a major fraction of the phytochromes at equilibrium. **c,** Relative rate of recruitment under various wavelengths of light of approximately equivalent intensity as determined by cytoplasmic depletion. Blue light is nearly two orders of magnitude less efficient at inducing phytochrome activation than red light.

Following Rac1 activation by recruited TIAM DHPH with a TIRF Recruitment Biosensor
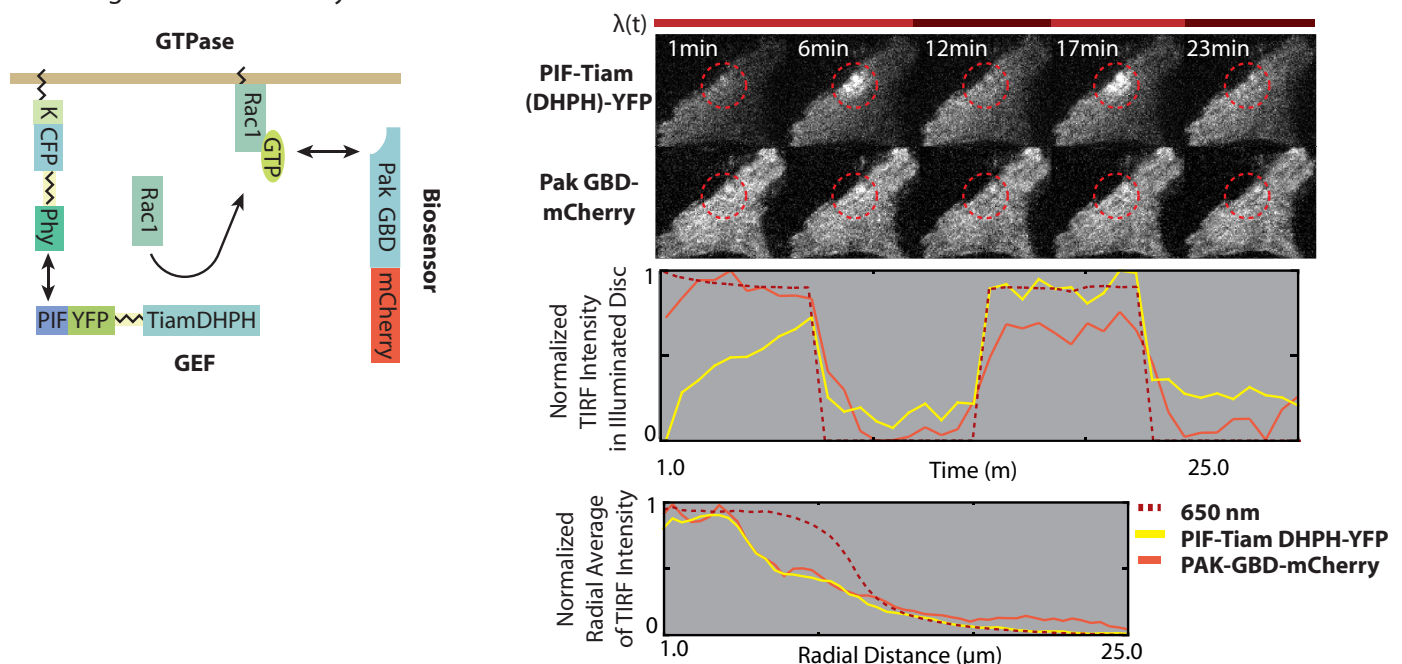
Figure S4 Response dynamics of Rac1-GTP monitored by use of a TIRF recruitment biosensor. Left panel depicts the activation (nucleotide exchange) of Rac1 to its active, GTP-bound form. mCherry-labelled PAK GBD domain binds specifically to the GTP-bound form of Rac1 and is thereby concentrated near localized sources of GEF activity. Microscopy panels show TIRF images of Tiam DHPH-YFP-PIF and PAK-GBD-mCherry. The PAK-GBD-mCherry increase at the point of red-light activation is subtle visually but easily followed by tracing the integrated intensity of the region. Plots show the overall rapid behavior in time within the illuminated region as the red light is turned on and off and the relative spatial distribution of DHPH and sensor during the first "activation peak".

Estimates for in-vivo PIF6-PhyB Kd assuming
nM to mM concentrations of PIF3,PIF6,PhyB
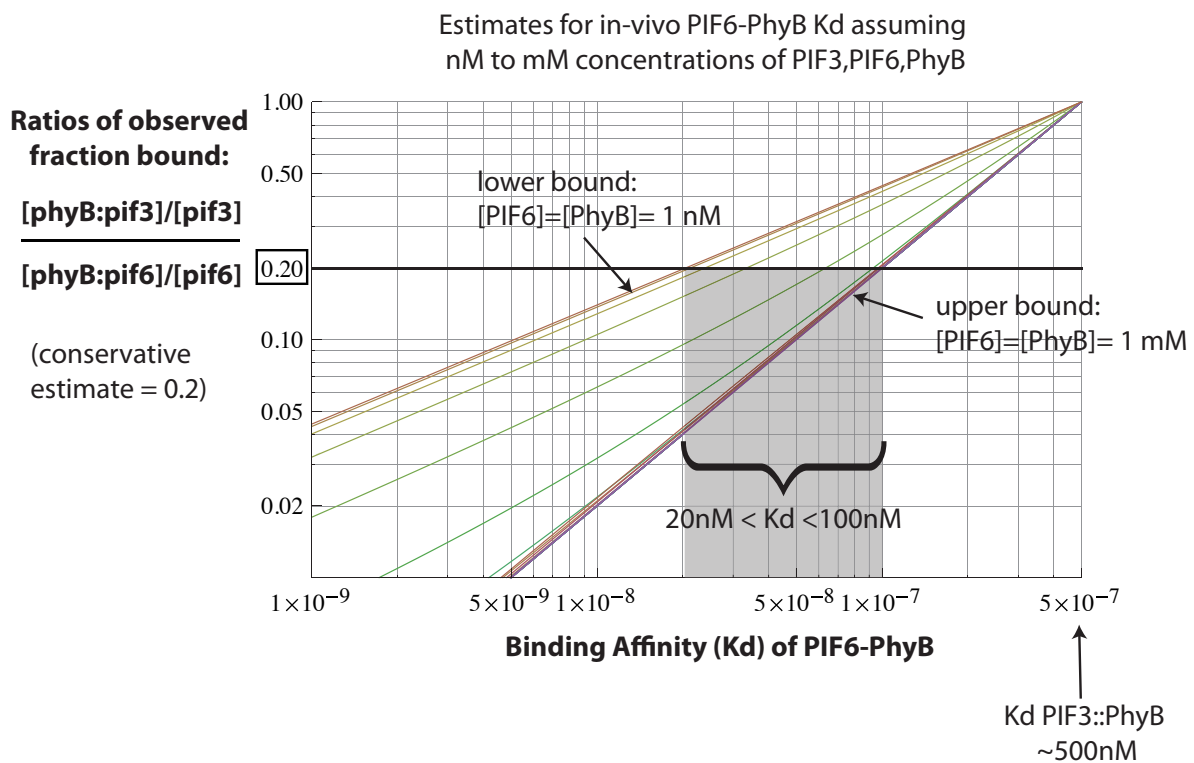
Figure S5 Conservative bounds for the Kd for the PIF6::PhyB interaction can be obtained by comparing the experimental membrane/cytoplasmic fraction ratios of YFP-PIF6 and YFP-PIF3 from identical experimental designs. The steady-state recruitment levels depend on few parameters: 1) the total concentration of membrane-localized phytochrome, 2) the total concentration of cytosolic PIF-YFP, 3) the Kd .
Assuming equal physiological concentration ranges, we can compare relative equilibrium recruitment levels to bound the relative Kds. Even overestimating the baseline degree of PIF3-PhyB recruitment to be 50% and underestimating the recruitment level of PIF6-PhyB to be only 84% yields a relative Kd[pif6:phyB908]/Kd[pif3:phyB908] that is 5-10x fold lower. Using the previously measured value of ~500nM for PIF3::PhyB, our interaction's Kd would then be bounded below 100-50nM.